Journal of Physics B:
Atomic, Molecular and
Optical Physics

Low energy elastic and inelastic scattering of positrons from formic acid

OPEN ACCESS
IOP Publishing
Journal of Physics B: Atomic, Molecular and Optical Physics
J. Phys. B: At. Mol. Opt. Phys. **57** (2024) 175201 (7pp)
https://doi.org/10.1088/1361-6455/ad636a

Low energy elastic and inelastic scattering of positrons from formic acid

D Stevens[1], Aaditya Datar[2], Z Cheong[1] and J P Sullivan[1,*]

[1] Positron Research Group, Research School of Physics, Australian National University, Canberra ACT 2601, Australia
[2] Department of Physics, Indian Institute of Science Education and Research, Homi Bhabha Road, Pashan, Pune 411008, India

E-mail: james.sullivan@anu.edu.au

Received 9 April 2024, revised 20 June 2024
Accepted for publication 15 July 2024
Published 26 July 2024

Abstract

This paper presents a detailed study of low energy positron scattering from formic acid, examining elastic scattering, electronic excitation and ionisation processes. Through detailed comparisons with previous experimental and theoretical data, it is clear that the picture for positron scattering from this target remains incomplete, with significant disagreement between experiment and theory in the comparisons of differential cross section data. Calculations of elastic electron scattering are unexpectedly in better agreement with the positron scattering experiments, and give some hints as to potential areas for improvement in the modelling of scattering for targets which tend to be dominated by dipole interactions.

Keywords: positron scattering, formic acid, low energy, electron scattering, differential cross section

1. Introduction

Positrons are a tool for the investigation of fundamental scattering physics, as well as having application in technologies such as Positron Emission Tomography (PET) [1]. In addition, the emerging techniques of positherapy [2] and theranostics [3] use *in vivo*, positron emitting radioisotopes and will broaden the use of positrons in health-based applications. There is, in fact, significant cross over between the fundamental and applied uses, as a better understanding of the interactions of positrons inside the human body can inform potential improvements in the understanding and application of PET scans, in particular the quantification of radiation damage at the tail end of the positron thermalisation pathway. Models have been developed to take gas phase scattering cross sections and apply them to calculate positron transport in liquids [4, 5], for instance, which then stand as a proxy for the interactions in human tissue. There have been a range of measurements of positron scattering from different biomolecules (e.g. [6–11]), with the intention of building a database of positron interactions that can serve as inputs into models that increase the level of sophistication of the description of low energy positron transport, as well as benchmarks for the theoretical description of positron scattering from more complex molecules.

In this paper, we present measurements of positron scattering from formic acid (HCOOH), focussing on the elastic scattering, electronic excitation and ionisation processes. Formic acid is the simplest organic acid and is one of the building blocks of more complex molecular structures that are found in biological systems, with the formate group (–COOH) found across an array of bigger amino acids and other biomolecules. Previous experimental groups have studied positron scattering from this target, mainly focussed on measuring grand total cross sections [12–14]. Makochekanwa *et al* [14] also presented the total positronium formation cross section and the so-called 'grand total minus positronium formation' cross section

* Author to whom any correspondence should be addressed.

(GT-Ps), which below the onset of ionisation can be thought of as a reasonable approximation to elastic scattering. The paper of Zecca *et al* [13] included Schwinger multichannel (SMC) calculations of elastic positron scattering up to 10 eV impact energy.

There have been a range of electron scattering measurements and calculations for interactions with formic acid. Of particular relevance to this work are the differential cross section (DCS) measurements of Vizcaino *et al* [15], and the calculations of this process by Trevisan *et al* [16]. We note that there are also calculations of electron elastic differential scattering by Gianturco and Lucchese [17].

Formic acid has a permanent dipole moment of 1.41 D, and also a large dipole polarisability of 22.5 a.u., and can exist in one of two stable conformers. The *cis* and *trans* form are separated by 169 meV in the gas phase, and the calculation of the Boltzmann population distribution gives a strong preponderance of the *trans* form at room temperature. Depending on the pressure, formic acid will additionally form dimers for some percentage of its gas phase population. For the pressures used in this work, the percentage of dimers present is less than a few percent across all measurements, and thus has a very small influence on the resulting cross sections. The first electronic excited state for the molecule is the $1\ ^1A''$ state, with an excitation energy of 5.91 eV from the ground state [18]. This state is only very weakly excited by photon impact, however, and thus it might be more relevant to consider the $2\ ^1A'$ transition, with an energy of 7.53 eV, as the first state relevant for positron scattering. The ionisation threshold is at 11.33 eV for this target, with a corresponding positronium formation threshold of 4.53 eV.

2. Experimental procedure

The measurements presented here were made on a Surko trap and beam system [19, 20], located at the Australian National University. Both the experimental system [21] and the analysis techniques [22] are well established, so only a brief description of the process follows here. Positrons from a ^{22}Na source are moderated using solid neon, with the low energy beam that results confined radially by a ∼500 G magnetic field. They are then directed into the Surko trap, where they are trapped and cooled using a combination of electrostatic fields and a N_2 and CF_4 buffer gas mixture. The result is a positron cloud cooled to the gas (room) temperature, which then forms the basis of a pulsed positron beam. This beam has a narrow energy spread, of between 40 and 100 meV (FWHM) for the measurements presented here, which was directed to a gas cell containing the formic acid.

The formic acid was obtained from the vapour pressure above a liquid sample. Before use in the experiment, the sample went through several freeze-pump-thaw cycles to expunge any trapped gases and ensure high target purity. Gas was then admitted to the gas cell through a needle valve, and the pressure inside the cell measured using a high accuracy capacitance manometer. Positrons passing through the cell interact with the target and these interactions cause a spread in the parallel energy component of the magnetically confined beam. This energy spread can then be analysed using a combination of a retarding potental analyser and microchannel plate detector. This information about the scattering processes is then combined with knowledge of the scattering cell length and vapour pressure, allowing us to obtain absolute cross section values for a variety of scattering processes [22, 23].

Table 1. Missing angular range for forward scattered elastic positrons in the present elastic total cross section measurements.

Energy (eV)	Minimum angle (deg)
1	14
2	10
5	9
10	7
20	5

When inelastic scattering is present, additional consideration is required to separate out the elastic and various inelastic components. This is done by changing the ratio of the magnetic field between the gas cell and the analysing stage of the experiment, to distinguish energy loss from angular scattering [22]. In the case of these measurements, a ratio of 4 was used, which in turn limited the energy range of the measurements to 20 eV, in order to be able to successfully separate elastic scattering, electronic excitation and ionisation. Note that due to the energy spread of the beam, rotational and vibrational excitations are not able to be resolved, and so cross sections are presented as a sum over rotational and vibrational modes. The energy resolution also provides a limit on the ability to separate elastic forward angle scattering from the incident positron beam. Thus the measurement of the total elastic scattering is only a lower bound, with the portion of forward angle scattering missed indicated in table 1. Elastic DCS also have a correspondingly limited angular range of measurement. The DCS are folded around 90°, due to the reflection of backscattered positrons and their retransmission through the scattering cell. Re-scattering is limited by maintaining the scattering percentage within the cell to less than 10% for the measurements presented here, and thus this has a negligible effect on the final cross section values [22]. Comparisons are made to data that are similarly folded around 90°.

Uncertainty in the cross sections is dominated by the statistics of the measurement, but also includes small contributions from the pressure measurement (<2%) and uncertainty in the cell length (0.1%). All of the cross section values are normalised independently of other data and are given with absolute values and uncertainties.

3. Total elastic scattering

The present data for the total elastic scattering cross section (rotationally and vibrationally averaged) are compared to previous measurements and theory in figure 1, with tabulated values of our data given in table 2. Below the positronium formation threshold of 4.53 eV, the cross sections of [13] the present

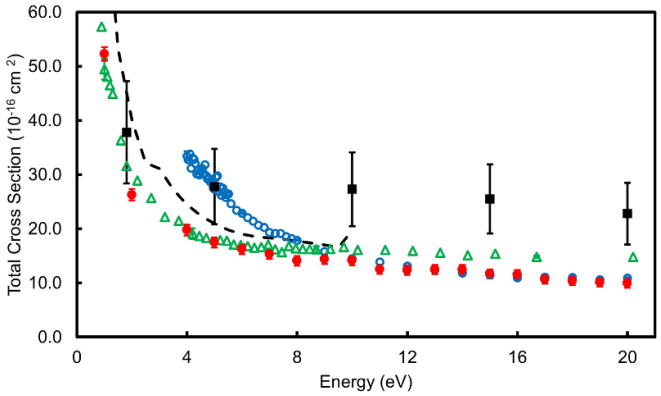

Figure 1. Total elastic cross section for positron scattering from formic acid. Solid red circles are the present experimental data, which are compared to previous measurements of the GT-Ps cross section (see text for details) from the same apparatus [14] (blue open circles), measurements by Zecca *et al* [13] (open green triangles) and SMC theory from the same paper (black dashed line). The black squares are the total elastic electron scattering cross section from [15], see the text for further discussion.

Table 2. Tabulated data for the total elastic scattering cross section for positron scattering from formic acid, in units of 10^{-20} m^2.

Energy (eV)	Elastic cross section (Å^2)	Error (Å^2)
1	52.29	1.28
2	26.29	1.06
4	19.77	0.99
5	17.48	0.95
6	16.26	0.93
7	15.32	0.91
8	14.08	0.90
9	14.38	0.89
10	14.18	0.89
11	12.53	0.87
12	12.38	0.87
13	12.46	0.86
14	12.45	0.86
15	11.69	0.83
16	11.54	0.84
17	10.72	0.84
18	10.40	0.84
19	10.16	0.83
20	9.94	0.83

data are effectively the same, measuring the elastic total scattering (integrated over vibrations and rotations). They are broadly in agreement, noting that the data of Makochekanwa *et al* have had a correction applied to allow for the missing forward angles in the scattering measurement, which substantially increases the overall magnitude. The data of Zecca *et al* have had no correction applied. The larger values of the Makochekanwa *et al* data in this energy range (and up to 8 eV) are reflective of the fact that the DCS used for these corrections is strongly forward peaked. Agreement between the present data and the Trento measurements (which are the grand total cross section, rather than elastic) continues up to around 10 eV, despite the opening of inelastic scattering such as positronium formation and electronic excitation processes. This suggests both that inelastic processes are small in magnitude and that the angular resolution of each apparatus is similar for the measurements presented here. Up to this energy, we can also compare to the SMC calculation [13] for the total elastic scattering. This curve lies higher than both sets of uncorrected data, again reflecting the missing forward angle scattering component. In general, this comparison might be expected and actually indicates a degree of consistency between theory and experiment. However, the correction applied to the data in [14] comes from the same calculation [24] and the corrected data lie significantly above the calculated total cross section. This suggests a discrepancy in the shape of the DCS between the theory and the experimental data. From 10 to 20 eV, the present data closely follow the GT-Ps results of [14], indicating that the dominant inelastic process in this energy region is positronium formation. The higher values of the experimental total cross section from Zecca *et al* in this region confirm this, as they also include all inelastic scattering processes in their measurement and lie somewhat higher in magnitude than the other two sets of positron scattering data.

We also compare the data in figure 1 with elastic electron scattering measurements from formic acid [15]. Here we can see that the total cross section is considerably larger at all energies than the present measurements. In this case, the total cross sections were obtained by extrapolating the DCS measured over an angular range of 10° to 130° using the complex Kohn variational theory of Trevisan *et al* [16]. This process takes into account the missing scattering angles from those measurements, which were then integrated to get the total cross section. The large error bars on this data predominantly reflect the uncertainty in the extrapolation.

4. Elastic differential scattering

Differential scattering cross sections allow us to probe greater detail in the scattering process. In figures 2 and 3 we present the current DCS measurements between 1 and 20 eV for the DCS of positron impact on formic acid. Tabulated data for these measurments is provided in table 3. As expected, figure 2 shows that the cross section magnitude drops from 1 to 4 eV, in line with the observations in the total cross section data. We can see that the DCS appears to be significantly forward peaked, which is consistent with the corrections to the data applied in Makochekanwa *et al*, which used the SMC theory of [13] as the basis for their correction. For energies between 5 eV and 20 eV, shown in figure 3, we see that there is less variation in both the shape and magnitude of the DCS, as might be expected given that there is minimal variation in the total cross section over this energy range. With the error margin of these measurements, any variation across the energy range is too small to discriminate with any certainty.

Figure 4 compares the current DCS data at 2 and 5 eV to SMC theory [13, 24] and to electron scattering data. In the case of electron scattering, the theoretical data of Trevisan *et al* [16] (in figure 4(b)) and the experimental data of Vizcaino *et al* [15] are in good agreement, and so for clarity we compare only

Table 3. Tabulated data for the present elastic DCS measurements. The cross sections are averaged over vibrational and rotational excitation (see text for details). Cross section units are 10^{-20} m^2 str^{-1}.

	1 eV		2 eV		4 eV		5 eV		10 eV		15 eV		20 eV	
Angle	DCS	Error	DCS	Error	DCS	Error	DCS	Error	DCS	Error	DCS	Error	DCS	Error
15							21.69	4.47	31.21	4.64	50.60	9.47	42.20	12.19
20	46.79	5.40	26.63	9.02	14.37	4.38	12.69	3.39	11.32	3.55	26.70	7.33	15.78	9.39
25	31.03	4.39	15.24	3.60	6.18	3.54	6.90	2.74	10.31	2.94	13.28	6.11	9.22	7.85
30	14.68	3.75	9.61	3.05	7.57	3.03	6.11	2.33	3.82	2.57	13.26	5.38	0.10	6.93
35	14.26	3.34	8.03	2.68	4.51	2.67	1.86	2.04	2.42	2.30	9.90	4.93	8.29	6.30
40	14.88	3.00	6.64	2.38	1.11	2.35	2.65	1.83	2.15	2.14	0.00	2.50	4.03	5.97
45	6.22	2.66	4.06	2.18	4.46	2.13	0.49	1.66	5.82	2.04	8.29	4.52	2.96	5.83
50	7.77	2.53	4.52	2.00	0.55	1.97	4.01	1.53	1.65	2.02	1.43	4.54	9.40	5.84
55	5.62	2.36	1.15	1.87	1.73	1.85	1.73	1.42	2.66	2.05	11.46	4.68	4.27	6.03
60	4.77	2.22	4.95	1.80	2.09	1.76	0.00	1.36	3.90	2.16	0.51	5.00	2.53	6.46
65	3.36	2.12	0.33	1.73	0.71	1.69	1.78	1.31	1.99	2.38	3.78	5.57	−2.79	7.16
70	3.58	2.07	2.92	1.66	1.18	1.63	0.92	1.26	3.34	2.76	7.34	6.61	5.14	8.51
75	0.08	2.06	1.03	1.64	0.32	1.58	0.75	1.23	3.49	3.48	6.03	7.34	0.79	10.92
80	2.06	2.19	6.17	6.28					3.52	5.03				

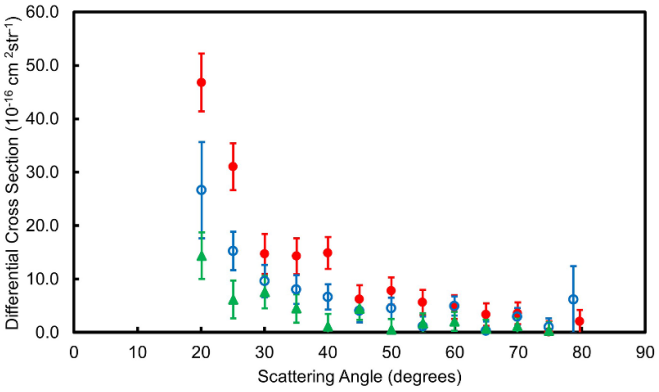

Figure 2. DCS measurements from formic acid at 1 eV (red solid circles) 2 eV (blue open circles) and 4 eV (green solid triangles.

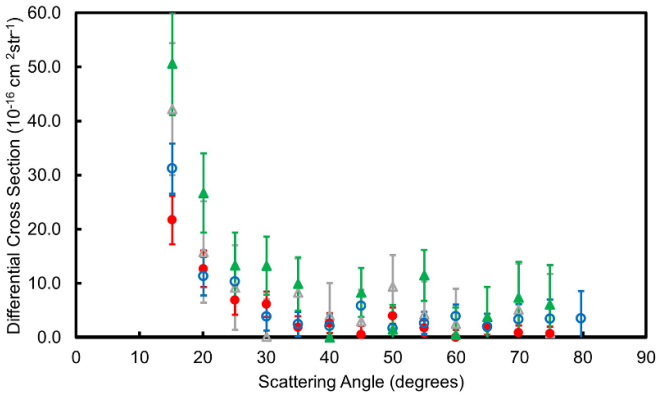

Figure 3. DCS measurements from formic acid at 5 eV (red solid circles), 10 eV (blue open circles), 15 eV (green solid triangles) and 20 eV (grey open triangles).

to the theoretical curve here. At 2 eV, in figure 4(a), we can see that the electron and positron DCS are almost identical, which suggests that the scattering is driven dominantly by polarisation effects (dipole moment and polarisability), which will be the same for each projectile. The agreement is surprisingly good, indeed, when considering that the theory predicts a negative ion resonance (albeit with a narrow energy width) at an energy of 1.9 eV. Given the agreement between positron and electron scattering, it is clear that any resonance feature at this energy has a very small effect on the DCS, which is a somewhat unexpected result. At the higher energy of 5 eV, in figure 4(b), we can compare to both electron scattering and the SMC theory calculation of positron scattering. It should be noted that this is just above the threshold for positronium formation (at 4.53 eV), which might be expected to have a small effect on the DCS but is not accounted for in the calculation. We can see that agreement is much better with the electron DCS than the positron calculation, although the experimental data is higher at the measured forward scattering angles than either theory. If polarisation is playing the dominant role in the low energy scattering processes, then there is some clear difference between the treatment in each scattering theory, with the Kohn variational technique handling this process better. However, both calculations are very complex, and discussion of possible material differences in the two is a topic for further investigation. What we can also note is the very steep rise in cross section values from the SMC calculation as the scattering angle goes to zero, which results from the Born closure technique applied in each calculation to deal with higher order partial wave contributions. These values continue to rise dramatically beyond the cutoff point shown in figure 4(b) (this is also true in the case of figure 5(a), discussed below). When used for correcting or extrapolating experimental data, as was the case in [14, 15] respectively, this may lead to an overestimation, with the precipitous rise and very low scattering angles contributing unrealistic amounts to the final integrated total cross section. This may go some way to explaining the difference between the electron scattering and positron scattering total cross sections, as seen in figure 1, and is a likely culprit in causing fortuitous agreement between experiment and

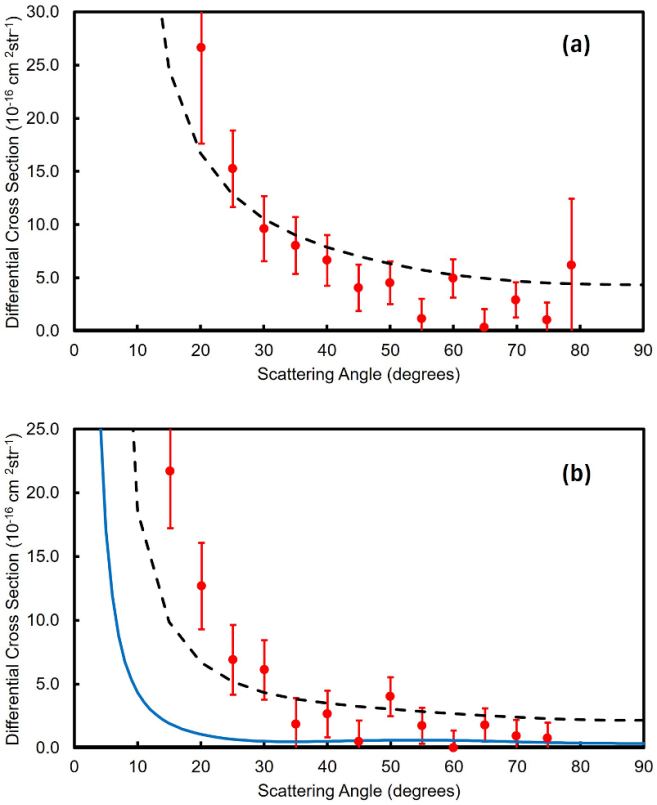

Figure 4. Present DCS measurements compared to theory and electron scattering at (a) 2 eV and (b) 5 eV. Red solid circles are the current experimental data, the blue solid line is the SMC calculation corresponding to the work in [13, 24] and the black dashed line are calculations of electron scattering at 2 and 5 eV from [16].

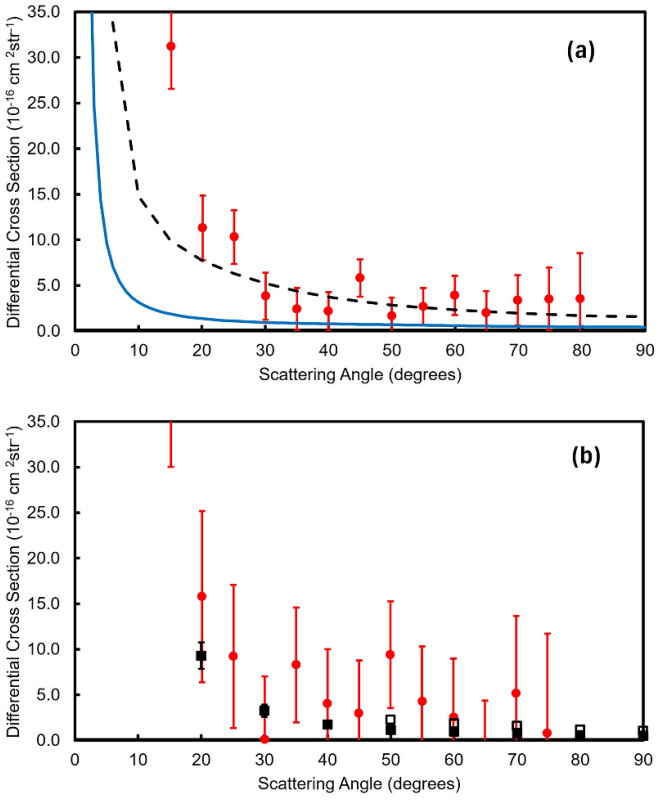

Figure 5. Present DCS measurements compared to theory and electron scattering at (a) 10 eV and (b) 20 eV. Red solid circles are the current experimental data, the blue solid line is the SMC calculation corresponding to the work in [13, 24], the black dashed line is a calculation of electron scattering at 10 eV from [16], solid black squares are the electron scattering measurements of [15], with open squares being the same data, folded around 90°.

theory at the total cross section level (see, for instance, Stevens *et al* [25]).

A similar comparison is made at higher scattering energies in figure 5. In this case, however, there is no theory for either positron or electron scattering at 20 eV and so in figure 5(b), we compare instead to the experimental data of Vizcaino *et al* [15]. Both the original data and data folded around 90 degrees are shown, although there are few points where the folding process is possible for the electron DCS in this case. Given the error bars on the present data, the consideration of the comparison is not affected. At these higher energies, the comparison is much the same as for 2 eV and 5 eV. We see that the positron scattering measurement is more forward peaked than either theory at 10 eV in the angular range of the measurement (however note that at low energies the SMC calculation increases dramatically, as previously discussed), with the electron scattering being a better match to the overall shape of the DCS. At 20 eV, there is no significant difference between the available positron and electron scattering data. For an impact energy of 10 eV electronic excitation is an open scattering channel, as is positronium formation for positron projectiles. It is then harder to make an argument that the sole difference between the theories is a difference in the treatment of polarisation effects—although the SMC calculation does not take into account positronium formation so both theories remain similar in basis. There is a clear disparity in the shapes between the two sets of positron scattering data, but in this case there is no reason to suspect that the electron scattering DCS should be particularly similar to positron scattering. Nonetheless, given the similarity in comparison at the lower energies, it appears that significant disagreement remains between experiment and theory at 10 eV, regardless of the role of positronium on the elastic scattering DCS. This also calls into question the magnitude of the correction applied in the case of the previous data from Makochekanwa *et al* [14], which relied on the SMC calculation to estimate the missing contribution from forward angle scattering.

5. Inelastic processes

In addition to elastic scattering, the use of the magnetic field ratio technique in the measurements [22] allowed the total electronic excitation and total ionisation (that is, direct ionisation, without a contribution from positronium formation)

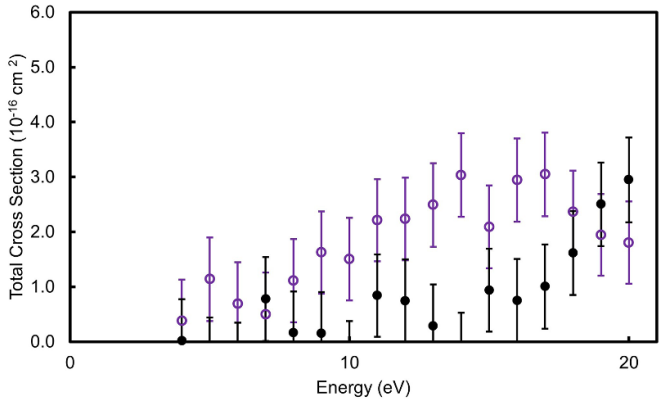

Figure 6. Total electronic excitation (open purple circles) and total (direct) ionisation (black circles) for positron impact on formic acid.

Table 4. Values of the total electronic excitation and total direct ionisation cross sections for positron impact on formic acid. Cross section units are given in 10^{-20} m^2.

Energy (eV)	Total inelastic	Error	Ionisation	Error
4	0.38	0.75	0.01	0.76
5	1.14	0.76	–0.32	0.76
6	0.69	0.76	–0.40	0.75
7	0.50	0.76	0.78	0.76
8	1.11	0.76	0.16	0.75
9	1.62	0.75	0.15	0.75
10	1.50	0.75	–0.39	0.76
11	2.21	0.75	0.84	0.75
12	2.23	0.75	0.74	0.76
13	2.49	0.76	0.28	0.76
14	3.03	0.76	–0.23	0.75
15	2.09	0.76	0.94	0.75
16	2.94	0.76	0.75	0.76
17	3.05	0.76	1.00	0.77
18	2.36	0.75	1.61	0.76
19	1.94	0.74	2.50	0.76
20	1.80	0.75	2.95	0.77

components of the scattering to be separated. Electronic excitation is averaged over all open electronic levels. The total cross sections for each process are shown in figure 6, with the corresponding data presented in table 4. In the case of electronic excitation, the cross section is zero to within the limits of the measurement until an energy of around 9 eV, after the threshold of the 2 ^{1}A′ excited state. This is in line with expectations, given that the lower energy 1 ^{1}A″ state is only very weakly excited by VUV photon impact [18]. The cross section rises to a maximum of about 3 Å^2 at an energy of approximately 15 eV and starts to fall off as the energy increases. At an energy of 10 eV, it is about 10% of the magnitude of the elastic scattering component, with a maximum contribution of about 25% of the elastic scattering at energies between 14 and 18 eV. Given the changing contribution of this scattering process across the energy range studied, as well as the likely effects of channel coupling, it is perhaps surprising that little effect is observed in the elastic DCS calculations, or indeed the measurements. Although it may be that a more detailed study needs to be pursued in the energy region where the contribution is greatest to come to any conclusions in this regard.

The total ionisation contributed very weakly in the energy region studied here, with a non-zero magnitude only being observed at energies above about 15 eV, as seen in figure 6. This is in line with expectations given the competing role of the positronium formation process in ionising the target, and comparison to the data in Makochekanwa *et al* [14] shows that it is only about 15 eV that the positronium formation cross section starts to decline after a sharp rise from the threshold of 4.53 eV. This is also consistent with many other previous observations of these two cross sections from a range of scattering targets (see, for instance, [6, 7, 26]).

6. Conclusion

Data is presented here for positron scattering from formic acid in the low energy region from 1 to 20 eV. Comparisons with previous data at the total cross section level show broad agreement, in particular when taking into account the limitations of the experimental measurements. However, DCS measurements show disagreement with the only current theory for this process, calculated using the SMC technique. Comparisons with electron scattering experiments show agreement over the range of angles mutually measured in experiment, but the broader angular range of calculations shows that the forward angle scattering is not properly accounted for in either positron (SMC) or electron (Kohn variational) scattering theories. It is speculated that at least part of the reason for disagreements is an incomplete description of the polarisation process in the models of scattering, given the permanent dipole moment and large dipole polarisability of the target along with the observation of strongly forward peaked DCSs. Measurements of electronic excitation suggest that the main contribution to this cross section in the current energy range comes from the 2 ^{1}A’ and higher energy states with no observable excitation of the recently observed 1 ^{1}A″ state [18]. The behaviour of the total direct ionisation cross section is consistent with previous observations and the fact that the positronium formation channel is the dominant ionisation process in this energy range.

Data availability statement

All data that support the findings of this study are included within the article (and any supplementary files).

Acknowledgments

This work was supported by the Australian Research Council through the Discovery Projects program, Grant Number DP190100696. Aaditya Datar would also like to acknowledge the support of the Future Research Talent Award fellowship provided by the Australian National University. The authors are grateful to Mr Ross Tranter for the ongoing technical support of the experimental activities. We would also like to thank Professor Cynthia Trevisan and Professor Marcio Bettega for

providing the tabulated theoretical data used in the comparison plots in this paper.

ORCID iDs

D Stevens https://orcid.org/0000-0001-6188-2682
Aaditya Datar https://orcid.org/0009-0003-8042-2325
J P Sullivan https://orcid.org/0000-0003-4489-4926

References

[1] Vaquero J J and Kinahan P 2015 Positron emission tomography: current challenges and opportunities for technological advances in clinical and preclinical imaging systems *Annu. Rev. Biomed. Eng.* **17** 385
[2] Moadel R M, Weldon R H, Katz E B, Lu P, Mani J, Stahl M, Blaufox M D, Pestell R G, Charron M J and Dadachova E 2005 Positherapy: targeted nuclear therapy of breast cancer with ^{18}F-2-Deoxy-2-Fluoro-d-Glucose *Cancer Res.* **65** 698
[3] Dijkers E C, Oude Munnink T H, Kosterink J G, Brouwers A H, Jager P L, de Jong J R, van Dongen G A, Schröder C P, Lub-de Hooge M N and de Vries E G 2010 Biodistribution of ^{89}Zr-trastuzumab and pet imaging of HER2-positive lesions in patients with metastatic breast cancer *Clin. Pharmacol. Ther.* **87** 586
[4] Tattersall W J, Cocks D G, Boyle G J, Brunger M J, Buckman S J, García G, Petrović Z L, Sullivan J P and White R D 2017 Spatial profiles of positrons injected at low energies into water: influence of cross section models *Plasma Sources Sci. Technol.* **26** 045010
[5] Boyle G J, Garland N A, McEachran R P, Mirihana K A, Robson R E, Sullivan J P and White R D 2024 Electron scattering and transport in simple liquid mixtures *J. Phys. B: At. Mol. Opt. Phys.* **57** 015202
[6] Cheong Z, Moreira G M, Bettega M H F, Blanco F, Garcia G, Brunger M J, White R D and Sullivan J P 2020 A comparison of experimental and theoretical low energy positron scattering from furan *J. Chem. Phys.* **153** 244303
[7] Edwards D, Stevens D, Cheong Z, Graves V, Gorfinkiel J D, Blanco F, Garcia G, Brunger M J, White R D and Sullivan J P 2021 Positron scattering from pyrazine *Phys. Rev.* A **104** 042807 accepted
[8] Palihawadana P, Boadle R, Chiari L, Anderson E K, Machacek J R, Brunger M J, Buckman S J and Sullivan J P 2013 Positron scattering from pyrimidine *Phys. Rev.* A **88** 012717
[9] Anderson E K *et al* 2014 Low energy positron interactions with uracil-total scattering, positronium formation and differential elastic scattering cross sections *J. Chem. Phys.* **141** 034306
[10] Chiari L, Palihawadana P, Machacek J R, Makochekanwa C, García G, McEachran R P, Brunger M J, Buckman S J and Sullivan J P 2013 Experimental and theoretical cross sections for positron collisions with 3-hydroxy-tetrahydrofuran *J. Chem. Phys.* **138** 074302
[11] Chiari L *et al* 2013 Total, elastic and inelastic cross sections for positron and electron collisions with tetrahydrofuran *J. Chem. Phys.* **138** 074301
[12] Kimura M, Sueoka O, Hamada A and Itikawa Y 1999 A comparative study of electron-and positron-polyatomic molecule scattering *Advances in Chemical Physics* (Wiley) pp 537–622
[13] Zecca A, Chiari L, Sarkar A, Lima M A P, Bettega M H F, Nixon K L and Brunger M J 2008 Positron scattering from formic acid *Phys. Rev.* A **78** 042707
[14] Makochekanwa C *et al* 2009 Total and positronium formation cross sections for positron scattering from water and formic acid *New J. Phys.* **11** 103036
[15] Vizcaino V, Jelisavcic M, Sullivan J P and Buckman S J 2006 Elastic electron scattering from formic acid (HCOOH): absolute differential cross-sections *New J. Phys.* **8** 85
[16] Trevisan C S, Orel A E and Rescigno T N 2006 Low-energy electron scattering by formic acid *Phys. Rev.* A **74** 042716
[17] Gianturco F A and Lucchese R R 2006 Electron scattering by formic acid in the gas phase: comparing measuredand computed angular distributions *Eur. Phys. J.* D **39** 399
[18] Randi P, Pastega D, Bettega M, Jones N, Hoffmann S, Eden S, Souza Barbosa A and Limão-Vieira P 2023 Electronically excited states of formic acid investigated by theoretical and experimental methods *Spectrochim. Acta* A **289** 122237
[19] Murphy T J and Surko C M 1992 Positron trapping in an electrostatic well by inelastic collisions with nitrogen molecules *Phys. Rev.* A **46** 5696
[20] Gilbert S J, Kurz C, Greaves R G and Surko C M 1997 Creation of a monoenergetic pulsed positron beam *Appl. Phys. Lett.* **70** 1944
[21] Sullivan J P, Jones A, Caradonna P, Makochekanwa C and Buckman S J 2008 A positron trap and beam apparatus for atomic and molecular scattering experiments *Rev. Sci. Instrum.* **79** 113105
[22] Sullivan J P, Gilbert S J, Marler J P, Greaves R G, Buckman S J and Surko C M 2002 Positron scattering from atoms and molecules using a magnetized beam *Phys. Rev.* A **66** 042708
[23] Machacek J R, Anderson E K, Makochekanwa C, Buckman S J and Sullivan J P 2013 Positron scattering from molecular hydrogen *Phys. Rev.* A **88** 042715
[24] Bettega M H F 2024 private communication
[25] Stevens D, Babij T J, Machacek J R and Sullivan J P 2022 Low energy electron scattering from pyridine using a surko trap and beam *J. Phys. B: At. Mol. Opt. Phys.* **54** 235202
[26] Boadle R A, Babij T J, Machacek J R, McEachran R P, Sullivan J P and Buckman S J 2016 Low-energy elastic and inelastic scattering of positrons from argon *Phys. Rev.* A **93** 022712